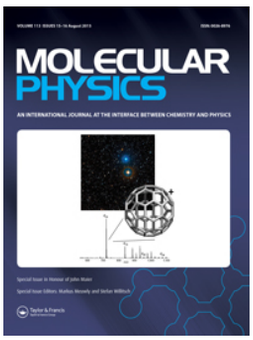

Taylor & Francis
Taylor & Francis Group

Molecular Physics

An International Journal at the Interface Between Chemistry and Physics

ISSN: 0026-8976 (Print) 1362-3028 (Online) Journal homepage: https://www.tandfonline.com/loi/tmph20

Adsorption of helium on isolated C_{60} and C_{70} anions

Martina Harnisch, Nikolaus Weinberger, Stephan Denifl, Paul Scheier & Olof Echt

To cite this article: Martina Harnisch, Nikolaus Weinberger, Stephan Denifl, Paul Scheier & Olof Echt (2015) Adsorption of helium on isolated C_{60} and C_{70} anions, Molecular Physics, 113:15-16, 2191-2196, DOI: 10.1080/00268976.2015.1018357

To link to this article: https://doi.org/10.1080/00268976.2015.1018357

Published online: 21 May 2015.

Molecular Physics, 2015
Vol. 113, Nos. 15–16, 2191–2196, http://dx.doi.org/10.1080/00268976.2015.1018357

Taylor & Francis
Taylor & Francis Group

INVITED ARTICLE

Adsorption of helium on isolated C_{60} and C_{70} anions

Martina Harnisch[a], Nikolaus Weinberger[a], Stephan Denifl[a], Paul Scheier[a] and Olof Echt[a,b,*]

[a]*Institut für Ionenphysik und Angewandte Physik, University of Innsbruck, Innsbruck, Austria;* [b]*Department of Physics, University of New Hampshire, Durham, NH, USA*

(*Received 28 November 2014; accepted 8 February 2015*)

Adsorption of helium on free, negatively charged fullerenes is studied in this work. Helium nanodroplets have been doped with fullerenes and ionised by electron attachment. For suitable experimental conditions, C_{60}^- and C_{70}^- anions are found to be complexed with a large number of helium atoms. Prominent anomalies in the ion abundances indicate the high stability of the commensurate 1×1 phase in which all hollow adsorption sites are occupied by one atom each. The adsorption energy for an additional helium atom is about 40% less than for atoms in the commensurate layer, similar to our previous findings for fullerene cations and in agreement with theoretical dissociation energies. Similarly, an anomaly in the adsorption energy occurs when 60 helium atoms are attached to C_{60}^- or 65 to C_{70}^-. For C_{60}, the anomaly coincides with the one observed for cationic complexes but for C_{70} it does not. Implications of these features are discussed in light of several theoretical studies of neutral and positively charged helium–fullerene complexes.

Keywords: doped helium nanodroplets; fullerenes; helium adsorption; adsorption energy; commensurate layer

1. Introduction

Physisorbed layers of atoms or molecules on corrugated surfaces exhibit a wide range of phenomena [1,2]. Graphite and its cousins graphene, nanotubes, and fullerenes are among the best studied surfaces [3], not least because of their potential for storage of hydrogen [4]. Another attractive feature of graphitic materials is the possibility to determine the effects of corrugation and adsorption energy, which depend on the curvature of the substrate and, for graphene, the number of carbon sheets.

At low temperatures physisorbed monolayers on graphite often form a variety of commensurate and incommensurate phases. Of interest are their structures, phase transitions, transition temperatures, and possible existence of structurally ordered phases in a second physisorbed layer. For ethylene, for example, seven different solid phases in the first layer have been reported [5]. The degree of order varies; some are commensurate and orientationally ordered, others are incommensurate and orientationally ordered or disordered.

Adsorption of helium and hydrogen adds another feature, the possible appearance of superfluidity. Up to seven distinct layers of helium form on graphite; several commensurate and incommensurate phases have been identified in the first layer at low temperature [2,6,7]. Structural order possibly extends to the second and even third layer [6,8].

The situation is different for graphene whose corrugation is weaker than that of graphite. Gordillo and Boronat have modelled ^{4}He on graphene with diffusion Monte Carlo methods and found that helium arranges in the $\sqrt{3} \times \sqrt{3}$ pattern (with helium atoms occupying the hollow sites of second-nearest carbon hexagons), but this solid phase is barely more stable than the liquid phase [9]. Markic et al., on the other hand, report that a helium cluster on graphene becomes more stable in the liquid phase than in the $\sqrt{3} \times \sqrt{3}$ phase if the graphene-mediated dispersion interaction, which weakens the He–He interaction, is included [10].

The convex surfaces of nanotubes and fullerenes offer stronger corrugation but weaker adsorption. In a series of experiments we have recently studied the adsorption of helium [11] and several molecular gases [12] on isolated C_{60}^+ and C_{70}^+ cations. Mass spectra indicate a strong energetic preference for formation of the 1×1 phase in which the 12 pentagons plus 20 hexagons of C_{60} (25 hexagons for C_{70}) are decorated with one particle each.

On planar graphitic surfaces, the 1×1 phase is not accessible because the distance between adjacent hollow sites is only 2.46 Å, much less than the equilibrium distance between helium, H_2, etc. in Van der Waals solids. On the other hand, the commensurate 1×1 layer of helium (or hydrogen) on C_{60} is underdense. Additional helium atoms can be accommodated although they displace atoms from hollow sites resulting in a layer that is either partially [11,13] or completely [14] liquid. Upon completion, the first layer becomes solid but it remains incommensurate [13,14].

* Corresponding author. Email: olof.echt@unh.edu

An obvious question is the adsorption capacity of this first layer. Our experimental data indicated that $He_{60}C_{60}^+$ and $He_{62}C_{70}^+$ contain complete layers. Theoretical studies agree that the adsorbate forms distinct layers as judged from radial distribution functions, but they differ in the value computed for the number of atoms in the first layer. In early studies, neutral C_{60} was treated as a sphere; the number of helium atoms in the first layer was found to be 65 [15] or 60 [16]. Later studies included the effects of corrugation. Shin and Kwon applied the path-integral Monte Carlo method and found that the first layer is filled at $n = 51$ [13]. Two other studies were devoted to cationic $He_nC_{60}^+$. Leidlmair *et al*. reported shell closure at $n = 74$ based on classical molecular dynamics; the value decreased to about 58 if quantum effects were included [11]. Calvo applied path-integral simulations and concluded that the first layer accommodates about 72 atoms [14]. Interestingly though, he observed that 60 atoms form a particularly rigid, incommensurate layer with a high adsorption energy while for most other sizes the layer formed a homogeneous fluid.

The present contribution explores adsorption of helium on negatively charged C_{60} and C_{70}. To the best of our knowledge this is the first study of adsorption on free fullerene anions. We find that the adsorption energy drops upon completion of the 1×1 phase nearly as much as for positively charged fullerenes, by about 40%. Furthermore, C_{60} anions and cations show the same anomaly in the dissociation energy at $n = 60$, which we had previously assigned to completion of the first adsorption layer. For $He_nC_{70}^-$ a weak but probably significant drop occurs at $n = 65$, three units above our previous result for $He_nC_{70}^+$.

2. Experimental details

Neutral helium nanodroplets were produced by expanding helium (Messer, purity 99.9999%) with a stagnation pressure of 24 bar through a 5 μm nozzle, cooled by a closed-cycle refrigerator (Sumitomo Heavy Industries LTD, model RDK-415D) to about 9.8 K, into a vacuum chamber (base pressure about 4×10^{-8} mbar). Droplets that form in the expansion contain an average number of 10^5 helium atoms [17]; the droplets are superfluid with a temperature of 0.37 K [18]. The resulting supersonic beam was skimmed by a 0.8 mm conical skimmer, located 8 mm downstream from the nozzle. The skimmed beam traversed a 20 cm long pick-up region consisting of two separate pick-up chambers [19]. Small amounts of C_{60} (MER, purity 99.9%) or C_{70} (SES, 99%) were vapourised at an oven temperature of 282 °C and 300 °C for C_{60} and C_{70}, respectively; the doped helium droplets were ionised by electron attachment at an energy of about 5.5 and 25 eV, respectively. The electron energy was varied in some experiments but it had no significant effect on the mass spectra.

Anions were accelerated into the extraction region of a reflectron time-of-flight mass spectrometer (Tofwerk AG, model HTOF) with a mass resolution $\Delta m/m = 1/3000$ (Δm = full-width-at-half-maximum). The base pressure in the mass spectrometer was 10^{-5} Pa. The ions were extracted at 90° into the field-free region of the spectrometer by a pulsed voltage. At the end of the field-free region they entered a two-stage reflectron, which reflected them towards a microchannel plate detector operated in single ion counting mode. Additional experimental details have been provided elsewhere [20].

Mass spectra were evaluated by means of a custom-designed software [21,22]. The routine includes automatic fitting of Gaussians to the mass peaks and subtraction of background by fitting a spline to the background level of the raw data. It explicitly considers isotopic patterns of all ions that are expected, i.e. in this work it accounts for contributions from ^{13}C (natural abundance 1.07%) to the $He_nC_m^-$ signal ($m = 60$ or 70). All isotopologues are included in the analysis. The abundance of specific ions (specific value of n) is derived by a matrix method.

3. Results and discussion

Mass spectra of anions formed by electron attachment to helium droplets doped with C_{60} or C_{70} are displayed in Figure 1(a) and 1(b), respectively. The prominent series of mass peaks that follow those of the bare fullerenes (off-scale) is due to ions with the composition $He_nC_m^-$ ($m = 60$ or 70). The insets show sections of the spectra (grey lines) together with Gaussian fits (red lines). The characteristic patterns of the isotopologues of C_{60} and C_{70} are clearly visible; isotopically pure $^{12}C_m$ forms the strongest mass peak in each group.

Impurities in the spectra are due to $H_2OC_m^-$ and C_{78}^-; other impurities that could not be identified are marked by x [panel (a)]. Visual inspection and, more systematically, the automatic data analysis routine (see Section 2) reveal a few other minor impurities by their distortion of the isotope pattern [for example at mass 895 u in panel (b)].

Other anomalies in the ion yield that are not caused by contamination are best seen in Figure 2, which displays the ion abundance of $He_nC_m^-$ (solid dots), extracted from the mass spectra by fitting Gaussians with due consideration of all isotopologues (see Section 2). Data points for sizes that show significant deviations from the expected isotope pattern have been omitted.

Prominent drops in the abundance of $He_nC_m^-$ occur after $n = 32$ and 37 for $m = 60$ and 70, respectively. These 'magic numbers' have been previously observed by our group in the studies of positively charged fullerene–helium complexes [11]; those data are included in Figure 2 as open dots. For $n < 60$, the size dependences of anions and cations are quite similar although there is more scatter in the anion data, probably due to poorer statistics.

The origin of magic numbers 32 and 37 is qualitatively well understood. On the surface of graphite or graphene

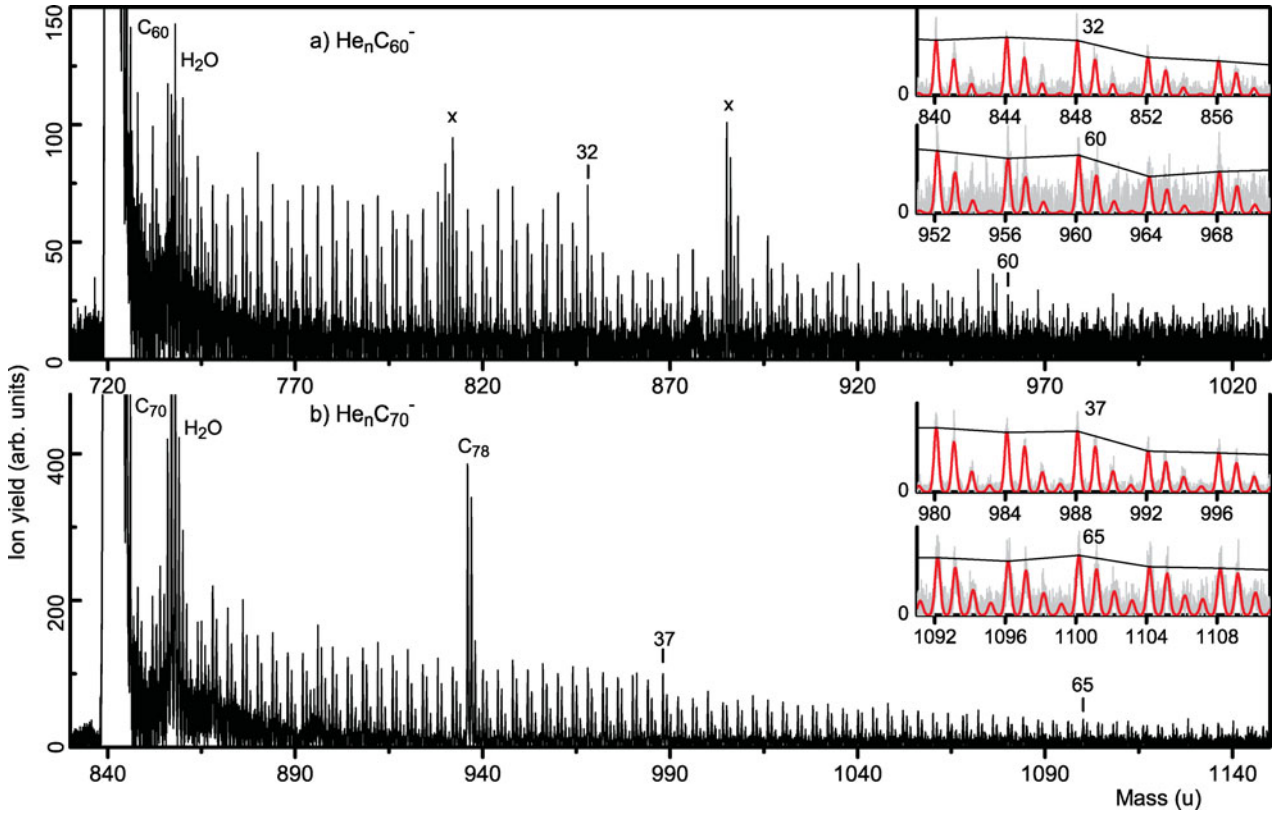

Figure 1. Negative ion mass spectra of helium droplets doped with C_{60} and C_{70} (panels (a) and (b), respectively). The insets display selected regions of the mass spectra (shown in light grey) together with fitted Gaussians (red lines). Straight lines connect mass peaks that correspond to the main (pure ^{12}C) isotopologues. Some mass peaks are labelled by the number of helium atoms n and some impurities are identified.

helium binds preferentially at hollow sites, above the centres of the hexagons of the honeycomb lattice. On planar graphite the distance between adjacent hollow sites is only 2.46 Å, too small for an adsorption layer where all hollow sites would be occupied (the so-called 1×1 phase). Instead, when the coverage equals 1/3 of the 1×1 phase (at 0.0637 helium atoms/Å^2) the $\sqrt{3} \times \sqrt{3}$ commensurate phase forms where all the second-nearest hexagon centres of the honeycomb lattice are occupied [6]. On graphene, which has a weaker corrugation than graphite, the situation is not as clear. The $\sqrt{3} \times \sqrt{3}$ solid phase competes with a two-dimensional superfluid phase [9,23]; the latter becomes more favourable than the commensurate phase if the graphene-mediated dispersion interaction between the helium atoms is included in the calculations [10].

The corrugation is stronger over curved convex surfaces [11]. At the same time, curvature increases the distance between atoms adsorbed at hollow sites to an extent that not only helium but even larger particles (including hydrogen, methane, ethylene or nitrogen) can be accommodated in the 1×1 phase of C_{60}, with one particle each at the centres of the 12 pentagons and 20 hexagons (25 hexagons for C_{70}) [19,22,24,25], for a review see [12]. The anomaly at $n = 32$ also appeared in mass spectra of C_{60} that was allowed to react in a gas aggregation cell with red phosphorous [26] or alkaline earth metals [27].

Anomalies in mass spectra point to anomalies in the stability of ions (see below for further discussion); they do not provide direct structural information. However, theoretical studies leave no doubt that 32 helium atoms form a commensurate 1×1 phase on neutral or positively charged C_{60} [11,13,14]. The same is true for adsorption of methane [24], ethylene [25], and xenon [28] but neither for neon, argon, and krypton [28] nor for polar molecules [29].

An incomplete layer of helium on C_{60}^+ is rigid, just like the 1×1 phase [11,13,14]. Even at a temperature of 4 K, which is the estimated temperature of the ions in our experiment [30], the single vacancy in the adsorbate layer of $He_{31}C_{60}^+$ remains localised over the full 5 ns duration of the simulation [11]. The situation changes drastically if the adsorbate layer contains more than 32 atoms. On fullerenes the 1×1 phase is of low density; it leaves room for additional helium atoms [11,13,14]. Additional atoms will displace atoms from hollow sites but their radial distance from the C_{60} centre will only marginally increase [11]. Theoretical studies of He_nC_{60} (charged or neutral) do not agree

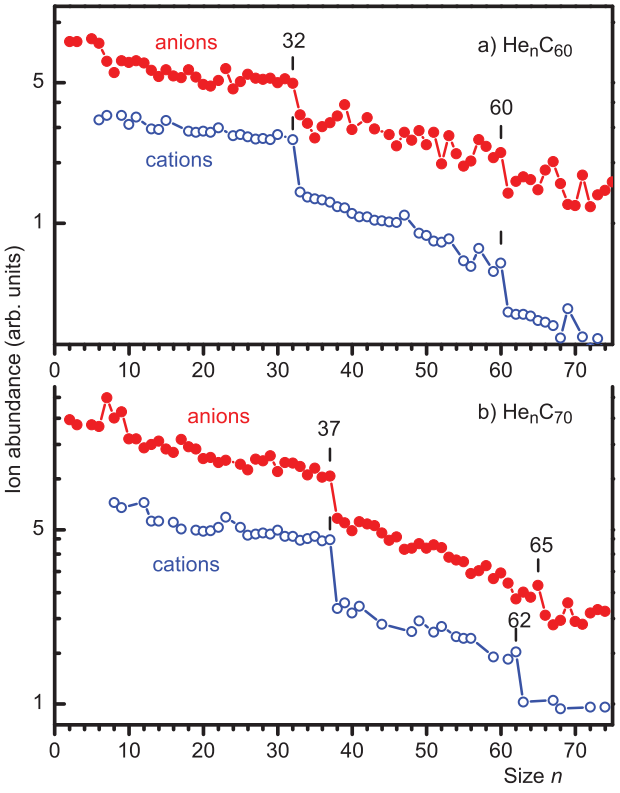

Figure 2. Semi-logarithmic plot of the abundance of $He_nC_{60}^-$ and $He_nC_{70}^-$ versus n (full dots in panels (a) and (b), respectively). Also shown (open dots) are the distributions of $He_nC_m^+$ cations ($m = 60$, 70) reproduced from reference [11].

on all details though. For example, in the classical molecular dynamics study by Leidlmair *et al*. the first atoms to be displaced are those at pentagonal sites; they form a fluid-like layer while atoms at hexagonal sites remain immobile [11]. On the other hand, the path-integral Monte Carlo simulation by Shin and Wong indicates that the first atoms to be displaced are those at hexagonal sites; atoms at pentagonal sites remain immobile [13]. In still another path-integral study, Calvo finds that the inclusion of zero-point motion in the harmonic approximation results in a helium layer that forms a homogeneous liquid for most values of n ($n > 32$) [14].

Our experimental data say nothing about these dynamic effects but they do carry quantitative information about the change in the adsorption energy as atoms are added. This information is presented in Figure 3(a) and 3(b) which show *relative* dissociation energies of He_nC_{60} anions and cations, respectively. As explained below, these quantities combine experimental ion abundances with theoretically determined dissociation (or evaporation or adsorption) energies D_n [11,32]. D_n is defined as

$$D_n = -E_n + E_{n-1}, \qquad (1)$$

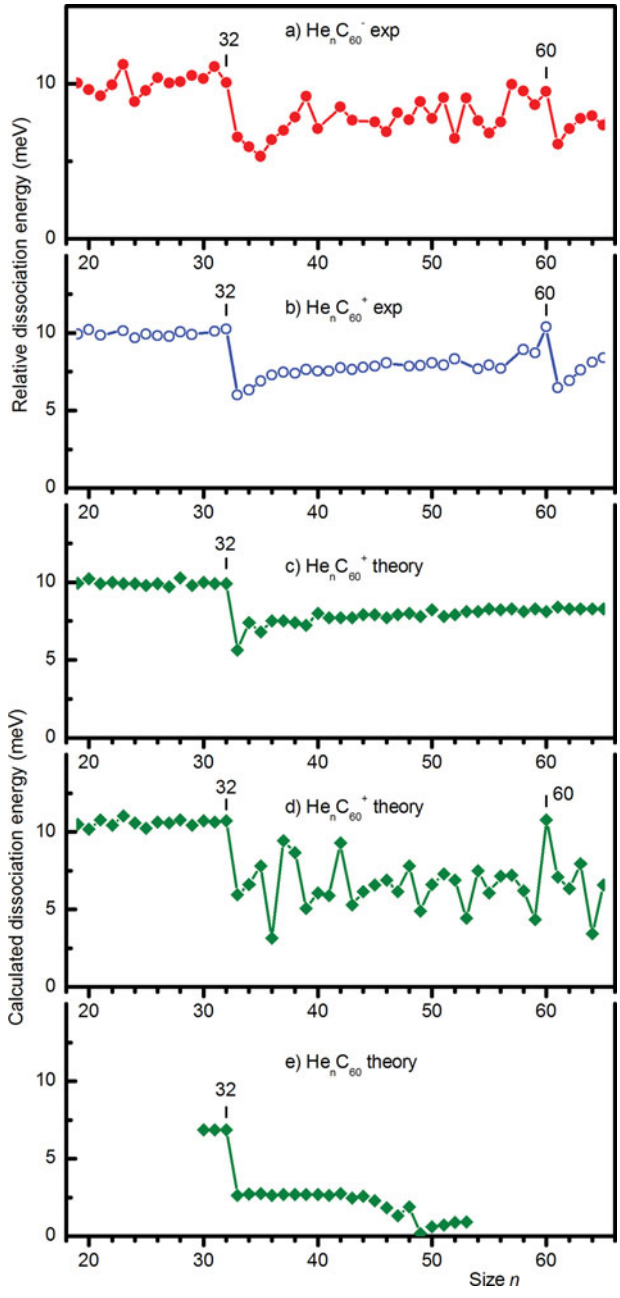

Figure 3. Relative dissociation energies of He_nC_{60} anions and cations (panels (a) and (b), respectively) derived from experimental data shown in Figure 2, and dissociation energies calculated for $He_nC_{60}^+$ (panel (c), from Ref. [11]). Also shown are dissociation energies calculated with path-integral simulation methods for $He_nC_{60}^+$ by Calvo [14] and for neutral He_nC_{60} by Shin and Kwon [13] (panels (d) and (e), respectively).

where E_n is the total energy of $He_nC_{60}^{\pm}$. Dissociation energies computed by Leidlmair *et al*. are displayed for $He_nC_{60}^+$ in Figure 3(c) [11]; the results of the two path-integral studies discussed above for $He_nC_{60}^+$ [14] and He_nC_{60} [13] are displayed in Figure 3(d) and 3(e), respectively.

Relative dissociation energies are derived as follows: first, the measured ion abundance is divided by a smooth function that describes the envelope of the data; this envelope depends on various experimental parameters and carries no information on energetics. The resulting spectrum is then multiplied by a smooth function that describes the envelope of dissociation energies D_n; we chose the dissociation energies of $He_nC_{60}^+$ computed by classical molecular dynamics shown in Figure 3(c) [11].

By design, the relative dissociation energies shown in Figure 3(a) and 3(b) have the same envelope as the theoretical data in Figure 3(c), and their size-averaged values are identical (close to 10 meV for $n \leq 32$). Local anomalies, however, truly reflect experimental information. This is evident from the striking difference between the anomaly at $n = 60$ in the experimental data (Figure 3(a) and 3(b)), which contrasts with the nearly constant values in Figure 3(c); this anomaly will be discussed further below.

In the vicinity of $n = 32$, the agreement between relative (experimental) and theoretical dissociation energies of $He_nC_{60}^+$ cations (Figure 3(b) and 3(c)) is excellent. Specifically, the adsorption energies are nearly constant until the commensurate layer is complete but the adsorption energy of the 33rd helium atom is 45% weaker; the values slowly recover as more atoms are added. For $He_nC_{60}^-$ anions, the drop in the relative dissociation energy beyond $n = 32$ is nearly as strong as for cations. This might have been expected because dissociation energies are not strongly affected by the polarity of the net charge; the classical adsorption energies of helium on neutral and cationic C_{60} agree within 4% [14].

The significance of several other anomalies in the anion data (Figure 3(a)) is questionable because of the considerable scatter but the second strongest anomaly, at $n = 60$, appears to be significant. It closely resembles the shape and strength of the anomaly in the cation data at $n = 60$, which we have attributed to completion of the first adsorption layer [11]. This agreement between anions and cations is surprising because, in contrast to the anomaly at $n = 32$ which is dictated by the number of carbon rings in C_{60}, the number of atoms in the complete adsorption layer is controlled by a subtle interplay of several factors including the helium–helium and helium–substrate interactions. This is perhaps best seen by comparing predictions of theoretical studies of helium adsorbed on C_{60}: values of $n = 65$ [15] and 60 [16] were derived in early theoretical studies of neutral C_{60} that omitted the effects of corrugation. More recent work included corrugation. Our classical molecular dynamics study of HeC_{60}^+ suggested completion of a layer at $n = 74$; the value changed to $n = 58$ upon including quantum effects [11]. From a path-integral study of $He_nC_{60}^+$ with correction for zero-point energy, Calvo concluded completion at $n = 72$ [14]. Interestingly, an anomaly in the dissociation energy was observed at $n = 60$ (but not 72) where a narrow minimum in the root-mean-square fluctuations of the adsorbate atoms indicated a solid phase. At the same time, the dissociation energy reached a local maximum as shown in Figure 3(d). Shin and Kwon reported a path-integral study of He_nC_{60} that included Bose permutation symmetry [13]. They observed completion of the first incommensurate layer at $n = 51$. At $n = 48$, however, a commensurate phase formed and the adsorption energy reached a local maximum, see Figure 3(e).

We are not aware of any theoretical studies of physisorption on C_{60} anions but some other recent work provides insight. The computed radial distribution of the difference in charge densities between C_{60}^- and C_{60} extends to about 6.8 Å [33], 0.5 Å beyond the maximum in the computed radial distribution of helium atoms adsorbed on neutral C_{60} [13]. The excess electron would thus be expected to weaken the adsorption energy and expand the solvation shell. However, it is less obvious how this would impact the number of helium atoms in the shell. In a naive geometric picture the shell may be expected to accommodate a larger number of atoms but the decrease in adsorption energy may have the opposite effect, as evident from a computer simulation of C_{60} solvated in ammonia [34]. For this system the adsorption energies of C_{60}^{z-} anions (z = even) are *larger* than for neutral C_{60}, the solvation shell *contracts* accordingly as z is increased from 0 to 6, and the number of NH_3 molecules in the shell changes in a non-regular fashion from $n = 47$ for $z = 0$ to 45 for $z = 2$ to 48 for $z = 6$.

We end with a brief discussion of adsorption on C_{70}. For cationic complexes we had previously observed a pronounced anomaly at $n = 62$, see Figure 2(b). The value was interpreted to indicate completion of the first layer, consistent with the value $n = 60$ for $He_nC_{60}^+$ because the ratio 60:62 agrees with the ratio that one would estimate for the size of a complete adsorption layer within a continuum approximation for C_{60} versus C_{70} (which has lower curvature). In our current work, we observe a small but probably significant anomaly at $n = 65$ for $He_nC_{70}^-$ (Figure 2(b)), three units above the one observed for cations. The highest occupied and the lowest unoccupied molecular orbitals in C_{60} are delocalised; the same is true of the HOMO and LUMO in C_{70} [35]. It is not obvious why there should be a large difference in the adsorption capacity between positively and negatively charged C_{70} if there is no such difference for C_{60}.

Conclusion

We have measured mass spectra of negatively charged fullerene–helium complexes. Anomalies in the abundance distributions allow us to estimate the change in the corresponding relative adsorption energies. A large decrease by about 40% occurs upon completion of the ordered 1×1 phase for $He_{32}C_{60}^-$ and $He_{37}C_{70}^-$; the decrease is nearly as large as for cations. Another prominent anomaly occurs

at $n = 60$ and 65 for C_{60}^- and C_{70}^-, respectively. A possible explanation of these numbers is the completion of the first adsorption layer but it is not clear why the number of atoms should depend on the charge polarity for C_{70} when there is no such dependence for C_{60}. Recent path-integral calculations of neutral and positively charged helium-C_{60} complexes [13,14] suggest that phenomena other than completion of the first layer may be responsible for the experimental observations.

Disclosure statement

No potential conflict of interest was reported by the authors.

Funding

This work was supported by the Austrian Science Fund, Wien [FWF project I978], [FWF project P23657], [FWF project P26635].

References

[1] W. Steele, Chem. Rev. **93**, 2355 (1993); L.W. Bruch, M.W. Cole, and E. Zaremba, *Physical Adsorption: Forces and Phenomena* (Oxford University Press, New York, 1997).
[2] L.W. Bruch, R.D. Diehl, and J.A. Venables, Rev. Mod. Phys. **79**, 1381 (2007).
[3] E.J. Bottani and J.M.D. Tascon, editors, *Adsorption by Carbons* (Elsevier Science, New York, 2008); S.M. Gatica and M.W. Cole, J. Low Temp. Phys. **162**, 573 (2011).
[4] A. Züttel and S. Orimo, MRS Bull. **27**, 705 (2002).
[5] W.A. Steele, Langmuir **12**, 145 (1996).
[6] D.S. Greywall, Phys. Rev. B **47**, 309 (1993).
[7] L. Reatto, D.E. Galli, M. Nava, and M.W. Cole, J. Phys. C **25**, 443001 (2013).
[8] P. Corboz, M. Boninsegni, L. Pollet, and M. Troyer, Phys. Rev. B **78**, 245414 (2008).
[9] M.C. Gordillo and J. Boronat, Phys. Rev. Lett. **102**, 085303 (2009).
[10] L.V. Markic, P. Stipanovic, I. Beslic, and R.E. Zillich, Phys. Rev. B **88** (2013).
[11] C. Leidlmair, Y. Wang, P. Bartl, H. Schöbel, S. Denifl, M. Probst, M. Alcamí, F. Martín, H. Zettergren, K. Hansen, O. Echt, and P. Scheier, Phys. Rev. Lett. **108**, 076101 (2012).
[12] O. Echt, A. Kaiser, S. Zöttl, A. Mauracher, S. Denifl, and P. Scheier, ChemPlusChem **78**, 910 (2013).
[13] H. Shin and Y. Kwon, J. Chem. Phys. **136**, 064514 (2012).
[14] F. Calvo, Phys. Rev. B **85**, 060502(R) (2012).
[15] E.S. Hernandez, M.W. Cole, and M. Boninsegni, Phys. Rev. B **68**, 125418 (2003).
[16] L. Szybisz and I. Urrutia, J. Low Temp. Phys. **134**, 1079 (2004).
[17] E.L. Knuth, U. Henne, and J.P. Toennies, presented at the 20th International Symposium on Rarefied Gas Dynamics, Beijing, 1996.
[18] J.P. Toennies and A.F. Vilesov, Angew. Chem., Int. Ed. Engl. **43**, 2622 (2004).
[19] C. Leidlmair, P. Bartl, H. Schöbel, S. Denifl, M. Probst, P. Scheier, and O. Echt, Astrophys. Astrophys. J. Lett. **738**, L4 (2011).
[20] H. Schöbel, P. Bartl, C. Leidlmair, S. Denifl, O. Echt, T.D. Märk, and P. Scheier, Eur. Phys. J. D **63**, 209 (2011).
[21] S. Ralser, J. Postler, M. Harnisch, A.M. Ellis, and P. Scheier, Int. J. Mass Spectrom., in press. doi:10.1016/j.ijms.2015.01.004
[22] A. Kaiser, C. Leidlmair, P. Bartl, S. Zöttl, S. Denifl, A. Mauracher, M. Probst, P. Scheier, and O. Echt, J. Chem. Phys. **138**, 074311 (2013).
[23] Y. Kwon and D.M. Ceperley, Phys. Rev. B **85**, 224501 (2012).
[24] S. Zöttl, A. Kaiser, P. Bartl, C. Leidlmair, A. Mauracher, M. Probst, S. Denifl, O. Echt, and P. Scheier, J. Phys. Chem. Lett. **3**, 2598 (2012); ChemSusChem **6**, 1235 (2013).
[25] S. Zöttl, A. Kaiser, M. Daxner, M. Goulart, A. Mauracher, M. Probst, F. Hagelberg, S. Denifl, P. Scheier, and O. Echt, Carbon **69**, 206 (2014).
[26] F. Tast, N. Malinowski, M. Heinebrodt, I.M.L. Billas, and T.P. Martin, J. Chem. Phys. **106**, 9372 (1997).
[27] U. Zimmermann, N. Malinowski, A. Burkhardt, and T.P. Martin, Carbon **33**, 995 (1995).
[28] S. Acosta-Gutierrez, J. Breton, J.M.G. Llorente, and J. Hernandez-Rojas, J. Chem. Phys. **137**, 074306 (2012).
[29] S. Denifl, F. Zappa, I. Mähr, F. Ferreira da Silva, A. Aleem, A. Mauracher, M. Probst, J. Urban, P. Mach, A. Bacher, O. Echt, T.D. Märk, and P. Scheier, Angew. Chem. Int. Ed. Engl. **48**, 8940 (2009); S. Denifl, F. Zappa, I. Mähr, A. Mauracher, M. Probst, J. Urban, P. Mach, A. Bacher, D.K. Bohme, O. Echt, T.D. Märk, and P. Scheier, J. Chem. Phys. **132**, 234307 (2010); H. Schöbel, C. Leidlmair, P. Bartl, A. Aleem, M. Hager, O. Echt, T.D. Märk, and P. Scheier, Phys. Chem. Chem. Phys. **13**, 1092 (2011).
[30] The temperature of clusters in an evaporative ensemble is proportional to their binding energy [31]. Undoped helium droplets cool to 0.37 K [18]; their binding energy (0.62 meV) is an order of magnitude weaker than that of $He_nC_{60}^+$.
[31] C.E. Klots, Nature **327**, 222 (1987).
[32] L. An der Lan, P. Bartl, C. Leidlmair, R. Jochum, S. Denifl, O. Echt, and P. Scheier, Chem. Eur. J. **18**, 4411 (2012).
[33] S. Klaiman, E.V. Gromov, and L.S. Cederbaum, Phys. Chem. Chem. Phys. **16**, 13287 (2014).
[34] C.A. Howard and N.T. Skipper, J. Phys. Chem. B **113**, 3324 (2009).
[35] C.A. Reed and R.D. Bolskar, Chem. Rev. **100**, 1075 (2000).